J|A|C|S COMMUNICATIONS

Published on Web 11/15/2010

Crystal Structures of Urate Bound Form of Xanthine Oxidoreductase: Substrate Orientation and Structure of the Key Reaction Intermediate

Ken Okamoto,[†] Yuko Kawaguchi,[†] Bryan T. Eger,[‡] Emil F. Pai,[‡,§,||] and Takeshi Nishino*,[†,⊥]

Department of Biochemistry and Molecular Biology, Nippon Medical School, 1-1-5 Sendagi, Bunkyou-ku, Tokyo 113-8602, Japan, Departments of Biochemistry, Medical Biophysics, and Molecular Genetics, University of Toronto and The Campbell Family Cancer Research Institute, University Health Network, Toronto, Ontario M5S1A8, Canada, and Department of Biochemistry, 1463 Boyce Hall, University of California, Riverside, 92521-0122, United States

Received September 7, 2010; E-mail: nishino@nms.ac.jp

Abstract: Two contradictory models have been proposed for the binding mode of the substrate xanthine to and its activation mechanism by xanthine oxidoreductase. In an effort to distinguish between the two models, we determined the crystal structures of the urate complexes of the demolybdo-form of the D428A mutant of rat xanthine oxidoreductase at 1.7 Å and of the reduced bovine milk enzyme at 2.1 Å, the latter representing a reaction intermediate. The results clearly indicate the catalytically relevant binding mode of the substrate xanthine.

Xanthine oxidoreductase (XOR) is a molybdenum-containing enzyme that catalyzes the hydroxylation of carbon atoms of a wide variety of substrates, including hypoxanthine and xanthine, which are the physiological substrates in many organisms.[1] Mammalian XOR is a homodimer of 290 kD molecular weight; each subunit contains one molybdopterin cofactor, two [2Fe−2S] centers, and one FAD molecule.[2] The oxidative hydroxylation of purine substrates takes place at the molybdenum center. Reducing equivalents introduced there are then transferred *via* two [2Fe−2S] centers to the FAD cofactor where reduction of the physiological electron acceptors occurs, NAD^+ in the case of the dehydrogenase form (XDH) or O_2 in the oxidase form (XO) of the enzyme occurs. In the oxidized form of XORs, the Mo(VI) ion is in the center of a square-pyramidal geometry, coordinated by an oxo- (═O) ligand at the apical position and one hydroxo (−OH) and one sulfido (═S) ligand at equatorial positions,[3a] in addition to the two vicinal sulfur ligands contributed by the pterin group (Figure 1a).

Crystallographic analysis of XOR complexed with the artificial substrate 4-[5-pyridine-4-yl-1*H*-[1,2,4]triazol-3-yl]pyridine-2-carbonitril (FYX-051) showed a mimic of the covalent intermediate of the hydroxylation reaction, in which the hydroxyl oxygen bridged the Mo-atom and the acceptor carbon atom of the aromatic ring of the substrate.[3a] This is consistent with a mechanism in which the side chain of a glutamic acid (1261 of the rat and bovine sequences), located near the Mo−OH, initiates catalysis by deprotonating the Mo−OH group as proposed previously for aldehyde oxidoreductase (AOR).[4] The free electron pairs of the oxygen then attack the electrophilic receptor carbon to yield the hydroxylated product. This leaves Glu1261 protonated; the formation of a hydrogen bond to the N-1 atom of the substrate stabilizes this state.[3] Its equatorial location appropriately positions the Mo═S ligand to accept a hydride ion from the reactive carbon atom to produce Mo−SH and a reduced Mo-center. The important contribution of this glutamic

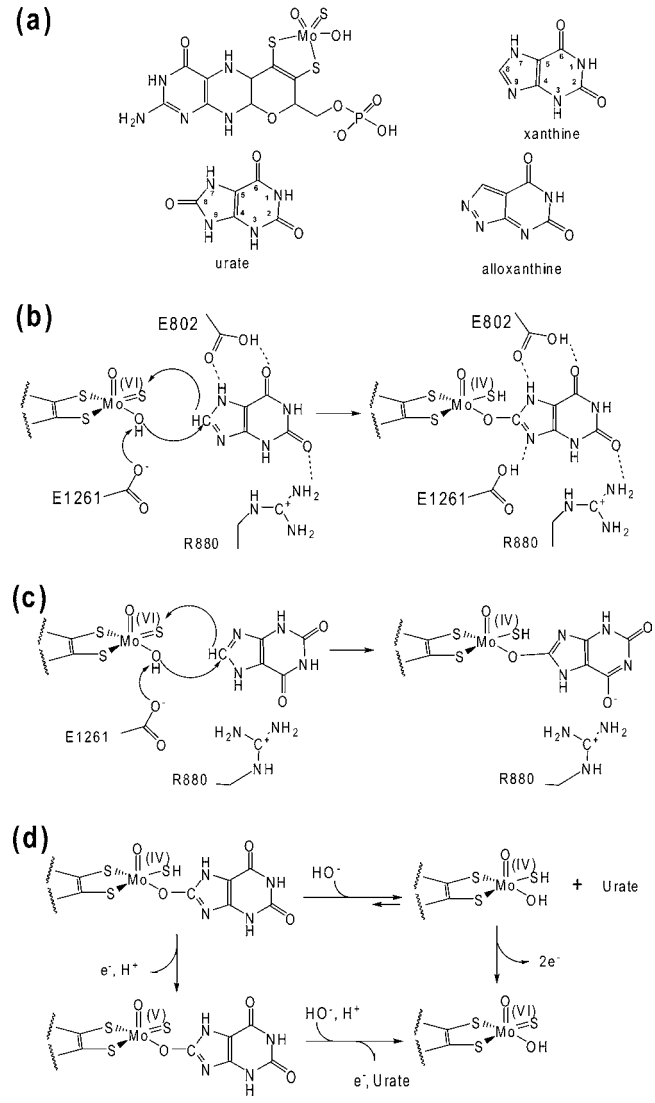

Figure 1. (a) Structures of molybdopterin, xanthine, alloxanthine, and uric acid. Reaction mechanism of XOR and binding modes of the substrate xanthine proposed by (b) Yamaguchi et al.[5] and (c) Pauff et al.[12] Amino acid numbers are those of bovine XOR. (d) Pathways of urate release from the intermediate.

[†] Nippon Medical School.
[‡] Department of Biochemistry, University of Toronto.
[§] Departments of Medical Biophysics and Molecular Genetics, University of Toronto.
[||] The Campbell Family Cancer Research Institute.
[⊥] University of California.

10.1021/ja1077574

acid residue to catalysis has been confirmed by mutating Glu1262 (Glu1261 in bovine XOR) in the human enzyme[5] and the corresponding Glu730 in *R. capsulatus* XOR.[6] The resulting proteins are devoid of any hydroxylation activity. Theoretical studies suggest that proton transfer from Mo—OH to the glutamic acid is induced upon binding of substrate.[7]

Currently of highest interest in the hydroxylation mechanism of XOR are the binding modes of the hypoxanthine and xanthine substrates as well as the exact roles that amino acid residues in the active site pocket play in facilitating the nucleophilic attack on the target carbon atom, electron transfer, and the subsequent release of product. A second glutamic acid residue (Glu802 in the bovine and rat sequences), located at the opposite side of the aromatic heterocycle-binding site, seems to be closely involved in purine substrate binding and transformation. The potent inhibitors, 2-(3-cyano-4-isobutoxyphenyl)-4-methyl-5-thiazolecarboxylic acid (TEI-6720, Febuxostat),[8] 1-[3-cyano-4-(2,2-dimethylpropoxy)phenyl]-1*H*-pyrazole-4-carboxylic acid (Y-700), and FYX-051, all settle in the narrow channel that connects the protein surface with the Mo-center. Their nonprotonated nitrogen atoms, which are important for the molecule's inhibitory potency, form hydrogen bonds to glutamic acid 802, suggesting that the carboxyl group is protonated. This residue interacts with the 4-oxo (O═) group of 4,6-dihydroxy-[4,4*d*]-pyrazolo-pyrimidine (alloxanthine) (Figure 1a).[10] When the corresponding glutamic acid in human XOR is replaced by a valine residue, the enzyme still displays activity with xanthine, albeit with a greatly reduced k_{cat}/K_m of around 1% of wild type. However, almost no turnover was observed for hypoxanthine.[5] In several crystallized complexes, the guanidinium group of Arg-880 (rat and bovine sequence) interacts with the carboxylate groups of the bound inhibitors[3a,8,9] and the 6-oxo (O═) group of alloxanthine.[10] This residue is conserved in all the XORs and AOR from *Desulfovibrio gigas* but is replaced by methionine in mammalian AORs.[11] In human XOR, contrary to what had been observed in the E803V mutant (Glu802 in bovine XOR), the R881M mutant (Arg880 in bovine XOR) still accepted hypoxanthine as a substrate, albeit again with greatly reduced activity (k_{cat}/K_m ~0.1% of wild type); xanthine hydroxylation was abolished.[5] Metabolic pathway studies indicated that prior 2-position hydroxylation (formation of xanthine from hypoxanthine) is crucial for hydroxylation at the 8-position (formation of uric acid from xanthine) to occur. Taking into account the alloxanthine complex crystal structure,[10] the catalytic importance of Arg880, and the involvement of the 2-position of xanthine, we proposed the binding mode of xanthine shown in Figure 1b, in which the various hydrogen bonding networks facilitate the nucleophilic attack by Mo—O^-. Another proposal suggested that an orientation, in which negative charge can be accumulated at the 6-position oxygen by having it interact with the positive charge of the guanidinium group of Arg880, would be energetically more favorable.[12] A classification scheme for bad (slow) (Figure 1b) and good (fast) (Figure 1c) substrates was proposed based on their orientation in the active site.[12] However, calculations using DFT[13] or QM/MM[14] techniques stated that the binding mode shown in Figure 1b is significantly more favorable than that in Figure 1c. Xanthine bound to native oxidized molybdo-enzyme cannot easily be trapped due to the ensuing fast reaction; an oxidized molybdenum center, on the other hand, quickly releases the product urate (Figure 1d). A medium resolution crystal structure of the catalytically inactive desulfo-form also could not with certainty define the relevant binding mode because the electron density could not be interpreted unequivocally, probably caused by superposition of various orientations, likely reflecting the wide substrate specificity of this enzyme.

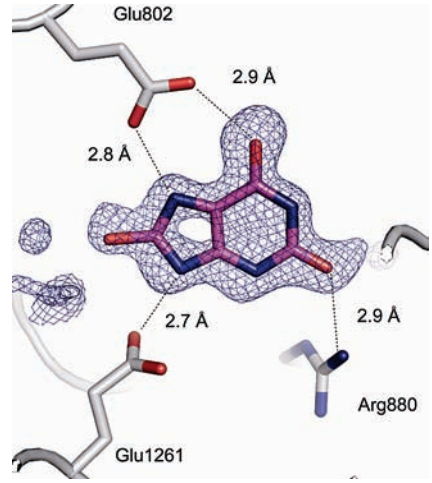

Figure 2. F_o-F_c electron density map of the active site of rat demolybdo-XOR D428A. The map was calculated with urate excluded from the refinement. The final model was superimposed onto the map contoured at 3.0 σ. Hydrogen bonds are shown as broken lines. Figure generated using Pymol.[15e]

Here, we present X-ray structures of the urate complexes of the demolybdo-form of the D428A mutant of rat XOR at 1.7 Å and of reduced bovine milk XOR at 2.1 Å resolution. The latter represents the catalytic intermediate of the xanthine to urate reaction. Rat XOR expressed in a baculovirus Sf9 insect cell system contains relatively large amounts of the demolybdo-form, which is in its normal protein conformation with all the cofactors, other than molybdo-pterin, at their proper place.[3b] HPLC analysis showed that the supernatant of a homogenate of Sf9 cells with 10 times their volume of suspension buffer contained micromolar concentrations of urate. The complex of demolybdo-XOR D428A and urate was purified and crystallized as previously described.[3b] The D428A mutant structure presented, which has the highest resolution among available rat XOR crystal structures, was generated to determine the role of Asp428 in the FAD reactivity of rat XOR. This residue lies close to the FAD cofactor far away from the molybdenum center, and its mutation did not affect the reactivity of the molybdenum center. The detailed analysis of this structure will be published elsewhere. Superimposition of the crystal structure of the molybdenum domain of this demolybdo-XOR with native bovine XOR showed that almost all the important amino acid residues of the demolybdo-form retain their orientation and position in the active site cavity (see Figure 3), presumably stabilized in their conformation by urate. Urate orientation in the rat demolybdo-XOR can be clearly identified from the electron density of the F_o-F_c map (Figure 2); it is consistent with the mode shown in Figure 1b; oxygen O6 and nitrogen N7 interact with Glu802 at hydrogen bond distances of 2.9 and 2.8 Å, respectively; nitrogen N9 binds to one of the carboxyl oxygens of Glu1261 (2.7 Å), and the NH atom of Arg880 contacts the 2-position of the purine ring (2.9 Å). The location of the carbon atom in position 8, which is to be hydroxylated, is almost identical to that of the corresponding atom of the FYX-051 covalent inhibitor, a mimic of a reaction intermediate. Therefore, one can argue that this structure closely reflects the binding mode of xanthine during hydroxylation, even so the molybdenum cofactor is absent and the 8-oxo atom, due to the sp2 hybridization of C8, assumes a position that would lie between the oxygen and sulfur ligands of the native molybdopterin.

We also tried to trap the structure of the reduced molybdenum cofactor bound to urate with the expectation of the OH group of Mo—OH being replaced by the C-8 oxo atom of urate (Figure 1d).

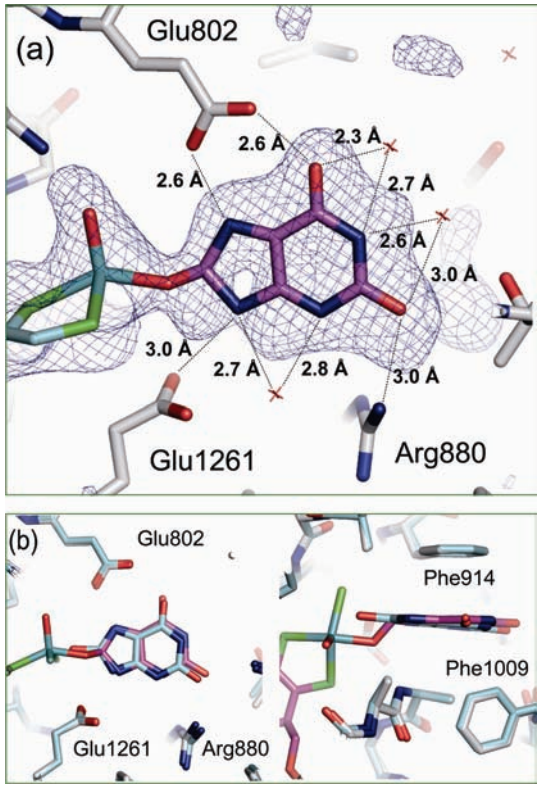

Figure 3. Atomic model of the active site of reduced bovine XOR with urate bound. (a) F_o-F_c electron density map contoured at 1.6 σ. To avoid model bias, the map was calculated before urate and molybdopterin molecules were included in the refinement. The final model was superimposed onto the map. Hydrogen bonds are shown as broken lines. (b) Superimposed views of urate bound to rat demolybdo-XOR D428A (carbon atoms are shown in cyan) and to reduced bovine XOR (protein carbon atoms are shown in gray, and carbon atoms in urate and molybdopterin are shown in magenta). The superposition was done with Cα atoms of the aa700−1300 of rat XOR and aa700−1301 of bovine enzyme. Cofactors were not included for the calculation. Figure generated using Pymol.[15e]

The crystal grown from highly active bovine XOR in its XDH form (prepared by folate affinity chromatography;[3c] activity/flavin ratio of 190) was soaked in a large excess of NADH under strictly anaerobic conditions in order to reduce both FAD cofactor and iron sulfur centers and to block any electron transfer from the Mo center. Then the Mo ions in the crystal were fully reduced by soaking in 4 mM titanium citrate[3a] solution followed by 250 μM urate. The crystal was cryo-cooled in liquid nitrogen, and data were collected at the Tsukuba photon factory synchrotron. Data were reduced with the program package HKL2000,[15a] and the structures determined by molecular replacement using the program MOLREP[15b] with salicylate-bound XDH (Protein Data Bank ID 1FO4) as a search model. The atomic model was built by using the program Coot,[15c] and refinement procedures followed standard protocols of the program CCP4, version 6.1.[15d] Water molecules were included and edited followed by the inclusion of urate and molybdopterin into the model. All relevant electron density maps were calculated before urate was added to the molecular model.

The electron density representing urate is lower, and the corresponding *B*-factors are higher than the values observed for the protein portion of the map. As the K_d of urate is assumed to be high, partial occupancy (estimated about 60%) is not surprising. The density, however, still allows reliable interpretation. The urate molecule locates near the Mo ion, and rather high electron density connects the two. This finding suggests a covalent linkage between molybdenum and urate *via* a bridging oxygen from urate. The bridging electron density is bent, spanning a total of 3.5 Å, and connects to the C8 atom of urate, the position where xanthine becomes hydroxylated in the course of the reaction. Placing the oxygen atom at the apex of the bent electron density leads to Mo−O and C8−O distances of 2.2 Å and 1.4 Å, respectively. The latter almost matches the standard C−O distance for a hydroxylated six-membered ring (1.3 Å) but is shorter than that reported for the 6-methyl-xanthine complex (1.6 Å).[12a] The oxygen is displaced from the C8−Mo axis toward the backbone amide of Ala1079 with a Mo−O−C angle of 116°. A distance of 2.3 Å for the equatorial Mo−S bond agrees with the sulfido ligand being in the Mo(IV)−SH form. As such, the structure presents a picture of arrested catalysis at the step of the intermediate formed in the course of oxygen atom transfer from the molybdenum coordination sphere to the substrate carbon to be hydroxylated.

Several hydrogen bonds and electrostatic interactions exist between the enzyme and the bound urate. Glu1261 in its protonated state forms a 3.0 Å long hydrogen bond to N9 of urate (Figure 3a). Glu802 is equidistant (2.6 Å) from both N7 and O=C6 of urate. In previous studies of XOR in complex with various inhibitors, arguments in favor of protonation of Glu802 have been presented.[3,8,9] A similar mode of interaction might also be seen in the present complex. Finally, the pyrimidine ring of urate is sandwiched between two phenylalanines, Phe914 and Phe1009 (Figure 3b), reminiscent of the binding of the aromatic salicylate ring to bovine XOR.[5] In addition, three water molecules (water 1889, 2106, 2338) are found within hydrogen bond distance to the pyrimidine ring. The distances between waters and the urate molecule are shown in Figure 3a.

The binding orientation of the urate portion of the intermediate is very similar to the one it assumes when bound to the demolybdo-form of the rat XOR D428A mutant. Superimposing the two urate-complex structures reveals that none of the amino acid residues interacting with urate, including the two glutamic acids, arginine, and two phenylalanines, move by more than 0.4 Å from each other (Figure 3b). The atoms of urate itself, however, are not completely overlapping; the C-8 oxo atom of urate bound to the demolybdo-form XOR is straight in the plane of the ring whereas it is attached to an sp^3-hybridized carbon, and therefore off the ring plane, when in the active site of the completely reduced XOR. However, the position of the C-8 carbon atom is the same in both cases, indicating that the binding mode of urate to the rat demolybdo-XOR D428A mutant resolved at high resolution mimics that of the reaction intermediate of the hydroxylation reaction of xanthine. Of the two models proposed for the binding mode of xanthine and its activation mechanism, the present X-ray structure analysis is only consistent with those shown in Figure 1b. Such an orientation not only explains molecular recognition between enzyme and substrate with ease but also is in agreement with previous theoretical studies that show that this orientation allows for nucleophilic attack by $Mo-O^-$ to form the intermediate Mo−O−C with assistance by hydrogen bond networks provided by active site amino acid residues.[13,14] As for most substrates the rate-limiting step in the catalysis by wild type XOR is likely the breakdown of the Mo−O bond accompanied by electron transfer and followed by release of the product;[16,3] the question of different stabilities of the Mo−O−C bond with different substrates will need further study.

Acknowledgment. This work was supported by Grant-in-Aid for Scientific Research 16205021 and 20590317 for Science Research from the Ministry of Education, Science, Sport and Culture of Japan and funded in part by the Canada Research Chairs Program. The synchrotron radiation experiments were performed

at beamlines BL17A and NW12A of the Photon Factory (Tsukuba); we are grateful to the beamline staff for their generous support.

Supporting Information Available: Statistics table of the crystallographic data (PDF). *B*-factors of urate, part of molybdopterin, amino acid residues and waters having hydrogen bonds with urate (PDF). $2F_o-F_c$ electron density maps of the active sites of rat demolybdo-XOR D428A and reduced bovine XOR with urate bound (PDF). This material is available free of charge via the Internet at http://pubs.acs.org.

References

(1) (a) Hille, R. *Chem. Rev.* **1996**, *96*, 2757–2816. (b) Hille, R. *Arch. Biochem. Biophys.* **2005**, *433*, 107–116. (c) Romao, M. J. *Dalton Trans.* **2010**, *21*, 4041–4260. (d) Nishino, T.; Okamoto, K.; Eger, B. T.; Pai, E. F.; Nishino, T. *FEBS J.* **2008**, *275*, 3278–3289.

(2) (a) Hille, R.; Nishino, T. *FASEB J.* **1995**, *9*, 995–1003. (b) Enroth, T.; Eger, B. T.; Okamoto, K.; Nishino, T.; Nishino, T.; Pai, E. F. *Proc. Natl. Acad. Sci. U.S.A.* **2000**, *97*, 10723–10728. (c) Garattini, E.; Mendel, R.; Romao, M. J.; Wright, R.; Terao, M. *Biochem. J.* **2003**, *372*, 15–32.

(3) (a) Okamoto, K.; Matsumoto, K.; Hille, R.; Eger, B. T.; Pai, E. F.; Nishino, T. *Proc. Natl.Acad. Sci. U.S.A.* **2004**, *101*, 7931–7936. (b) Nishino, T.; Okamoto, K.; Kawaguchi, Y.; Hori, H.; Matsumura, T.; Eger, B. T.; Pai, E. F.; Nishino, T. *J. Biol. Chem.* **2005**, *280*, 24888–24894. (c) Nishino, T.; Nishino, T.; Tushima, K. *FEBS Lett.* **1981**, *131*, 369–372.

(4) Huber, R.; Hof, P.; Duarte, R. O.; Moura, J. J.; Moura, I.; Liu, M. Y.; LeGall, J.; Hille, R.; Archer, M.; Romao, M. J. *Proc. Natl. Acad. Sci. U.S.A.* **1996**, *93*, 8846–8851.

(5) Yamaguchi, Y.; Matsumura, T.; Ichida, K.; Okamoto, K.; Nishino, T. *J. Biochem. (Tokyo)* **2007**, *141*, 513–524.

(6) Leimkühler, S.; Stockert, A. L.; Igarashi, K.; Nishino, T.; Hille, R. *J. Biol. Chem.* **2004**, *279*, 40437–40444.

(7) Amano, T.; Ochi, N.; Sato, H.; Sakaki, S. *J. Am. Chem. Soc.* **2007**, *129*, 8131–8138.

(8) Okamoto, K.; Eger, B. T.; Nishino, T.; Kondo, S.; Pai, E. F.; Nishino, T. *J. Biol. Chem.* **2003**, *278*, 1848–1855.

(9) Fukunari, A.; Okamoto, K.; Nishino, T.; Eger, B. T.; Pai, E. F.; Kamezawa, M.; Yamada, I.; Kato, N. *J. Pharmacol. Exp. Ther.* **2004**, *311*, 519–528.

(10) Okamoto, K.; Eger, B. T.; Nishino, T.; Pai, E. F.; Nishino, T. *Nucleosides, Nucleotides Nucleic Acids* **2008**, *27*, 888–893.

(11) Terao, M.; Kurosaki, M.; Demontis, S.; Zanotta, S.; Garattini, E. *Biochem. J.* **1998**, *332*, 383–393.

(12) (a) Pauff, J. M.; Hemann, C. F.; Jünemann, N.; Leimkühler, S.; Hille, R. *J. Biol. Chem.* **2007**, *282*, 12785–12790. (b) Pauff, J. M.; Zhang, J. J.; Bell, C. E.; Hille, R. *J. Biol. Chem.* **2008**, *283*, 4818–4824. (c) Dietzel, U.; Kuper, J.; Doebbler, J. A.; Schulten, A.; Truglio, J. J.; Leimkühler, S.; Kisker, C. *J. Biol. Chem.* **2009**, *284*, 8768–8776. (d) Cao, H.; Pauff, J. M.; Hille, R. *J. Biol. Chem.* **2010**, *285*, 28044–28053.

(13) Bayse, C. A. *Dalton Trans.* **2009**, *13*, 2306–2314.

(14) (a) Metz, S.; Thiel, W. *J. Am. Chem. Soc.* **2009**, *131*, 14885–14902. (b) Metz, S.; Thiel, W. *J. Phys. Chem. B* **2010**, *114*, 1506–1517.

(15) (a) Otwinowski, Z.; Minor, W. *Methods in Enzymology, Vol. 276, Part A*; Carter, C. W., Jr., Sweet, R. M., Eds.; Academic Press: New York, 1997; pp 307−326. (b) Vagin, A.; Teplyakov, A. *J. Appl. Crystallogr.* **1997**, *30*, 1022–102. (c) Emsley, P.; Cowtan, K. *Acta Crystallogr., Sect. D* **2004**, *60*, 2126–2132. (d) Collaborative Computational Project, Number 4: *Acta Crystallogr., Sect. D* **1994**, *50*, 760−763. (e) DeLano, W. L. *The PyMOL Molecular Graphics System*, 2002, http://www.pymol.org.

(16) (a) Schopfer, L. M.; Massey, V.; Nishino, T. *J. Biol. Chem.* **1988**, *263*, 13528–38. (b) McWhirter, R. B.; Hille, R. *J. Biol. Chem.* **1991**, *266*, 23724–23731.

JA1077574